Developing a framework for the assessment of current and future flood risk in Venice, Italy

by

J. Schlumberger (5001870)

to obtain the degree of Master of Science
in Hydraulic Engineering
at Delft University of Technology

Assessment committee:

Prof. Dr. ir. S.N. Jonkman	TU Delft, Hydraulic Structures and Flood Risk (chair)
Dr. ir. M. A. Diaz Loaiza	TU Delft, Hydraulic Structures and Flood Risk (supervisor)
Dr. ir. A. Antonini	TU Delft, Coastal Engineering
Dr. S. Fatorić	TU Delft, Architecture and the Built Environment
Dr. ir. C. Ferrarin	CNR-ISMAR

July 25, 2021

Contents

Cover image: Venetian during 12 November 2019 flood event. Source: Maria Grazia Beruffi, 2019 (accessed here: `http://www.aquagrandainvenice.it/en/imgs/46468`)

List of Figures

List of Tables

1 Abstract

Flooding has been a serious risk to the old-town of Venice, its residents and cultural heritage and continues to be a challenge in future. Despite this existence-defining condition, limited scientific knowledge on flood hazard and flood damage modelling of the old-town of Venice is available to support decisions to mitigate existing and future flood risk. Therefore, this study proposes a risk assessment framework to provide a methodical and flexible instrument for decision-making for flood risk management in Venice. It uses a state-of-the-art hydrodynamic urban model to identify the hazard characteristics inside the city of Venice. Exposure, vulnerability and corresponding damages are modelled by the multi-parametric, micro-scale damage model INSYDE transferred and adapted to the specific context of Venice with its dense urban structure and high risk awareness. A set of individual protection scenarios is implemented to account for possible variability of flood preparedness of the residents. The developed risk assessment framework was tested for the flood event of 12 November 2019. It was able to reproduce flood characteristics and resulting damages well. A scenario analysis based on the meteorological event like 12 November 2019 was conducted to derive flood damage estimates for the year 2060 for a set of sea level rise scenarios in combination with a (partially) functioning storm surge barrier MOSE. The analysis suggests that a functioning MOSE barrier could prevent flood damages for the considered storm event and all sea level scenarios almost entirely. It could reduce the damages by up to 34 % for optimistic sea level rise prognosis. Contrary, damages could be 1.08 to 5.92 times higher in 2060 compared to 2019 for a partial closure of the storm surge barrier depending on different levels of individual protection.

2 Introduction

Flood events are among the most disastrous natural catastrophes causing significant damages and fatalities all around the world. In Europe, coastal flood events are estimated to affect more than 100,000 citizens causing losses of about EUR 1.4 billion annually at present [1]. Under consideration of climate change scenarios, future flood damages are expected to increase due rising sea level [2].

In this context, hazard and flood risk assessment has been broadly implemented according to the 60/2007/EC directive in the EU [3]. According to the IPCC, flood risk is defined as the combination of a specific hazardous flood event, the exposure of human systems and their vulnerability, meaning predisposition to be adversely affected [4]. It can therefore consider adverse effects on human health, environment, cultural heritage and economic activities. As such, outcomes of a flood risk assessment framework can support systemic and individual decisions to mitigate flood damages or adapt accordingly, increase preparedness and strengthen coping capacities [5][6][7][8][9][10].

A flood risk assessment framework typically follows four steps: 1) hazard modelling, 2) assessment of vulnerability of exposed assets, 3) damage estimation and 4) flood risk estimation [11]. The application of 2D hydrodynamic models is current state of the art for deriving information about coastal and urban flood events [12][13][14][15][16]. Damage

modelling traditionally focuses on direct, tangible damages in terms of replacement costs related to structures, interior and public infrastructure as the cost-benefit analysis of flood mitigation measures is straight forward and indisputable [9][17][6][18][19]. The vulnerability of exposed assets is determined not only by the type of exposed structure, its construction material (quality), age and level of maintenance [20][21][9] but also by the level of present awareness; risk awareness influences the level of preparedness by means of physical measures (e.g. permanent or mobile water barriers, emergency works like sand bags) or behavioral adjustments (e.g. adapting the vertical distribution of goods and values). Vulnerability is therefore spatially and temporally highly varying [22][23][24].

This study focuses on the assessment of flood damage in Venice. The low-lying historic city has a long-lasting record of flood events [25] which is likely to extent in future mainly due to relative sea level rise and continuing subsidence [26][27][28][29][30]. Since 1987, the city of Venice is part of the UNESCO World Cultural and Natural Heritage site that spans the Venetian lagoon [31]. Consequently, not only economic and individual risk prevails, but also risk of damage or loss of highly valued cultural sites [32] which can be expected to contribute significantly to the tangible damages due to special restoration and reconstruction requirements [11]. Additionally, intangible damages to cultural heritage sites and their meaning for the cultural identity of the region and nation can be expected to further add to that [33].

Thus, dealing with flooding and mitigating adverse effects is an existence-defining task in Venice nowadays and in future. Over the past decades, flood protection mainly relied on the individual preparedness supported by forecasting systems for storm surges incorporated into a multi-stage warning system [34][27]. As part of an extensive flood protection plan, the Modulo Sperimentale Elettromeccanico (MOSE) barrier has been designed in the follow-up of the most extreme flood experienced in 1966. It is expected to be functional by the end of 2021. The barrier consists of a series of submersed gates located in the three inlets of the Venetian Lagoon. MOSE is designed to protect Venice against high water exceeding 110 cm ZMPS[1] up to a water level of 3.0 m ZMPS [35][36].

Despite much attention to flooding in the city of Venice, no detailed and methodical risk assessment framework is publicly available. Not having such a framework makes it more difficult to compare and evaluate various measures (such as MOSE barrier) and justify distribution of resources for flood risk mitigation measures [11]. Moreover, only a hand-full of studies on damage or loss modelling cover the old-town of Venice; some studies investigated potential flood damages based on basic depth-damage relations to analyse the benefit of a functioning barrier [37][38] or looked into remaining flood risk for floods up to a level of 110 cm ZMPS [39]. Other studies mainly focusing on different closure scenarios of the MOSE barrier consider flood risk implicitly by using a maximum safeguard water level at the city of Venice [35][36][40].

To develop a better understanding of the existing and future risk due to damages to structures and cultural heritage in Venice, a damage assessment framework is developed in this study as shown in figure 1. High resolution flood hazard characteristics

[1]If not highlighted otherwise, all levels refer to the local chart datum in Venice, given as Zero Mareographic of Punta della Salute (ZMPS), corresponding to the mean sea level of the 1885-1909 period. This reference is today 0.34 m below the present mean sea level (2019 annual mean sea level).

are computed by means of a 2D-hydrodynamic model. They feed into an adjusted version of the synthetic micro-scale damage model INSYDE to estimate expected absolute direct damages of the exposed buildings [18]. The flood model is calibrated and partly validated using the storm surge of 12 November 2019. Additionally, a damage claim data-set for the the same event is used for performance analysis of the damage model. Finally, the framework is applied to a set of scenarios of varying sea level change and MOSE closure to analyse potential development of flood damage in mid-term future.

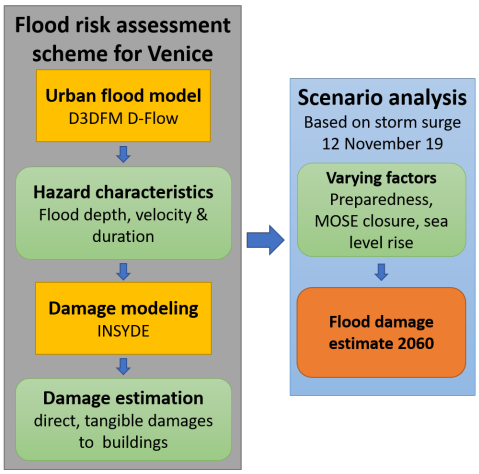

Figure 1: Risk assessment framework

The paper proposes a methodical and flexible assessment framework for Venice useful to analyse existing and future flood damages for different meteorological storm events. It is methodical, as it uses a hydrodynamic model along with a damage model that allows to resolve physical damage modelling of separate building components. The framework is flexible because both models can be refined to consider additional elements of influence or additional elements at risk. This could be of particular interest for accounting more specific conditions of cultural heritage as well as incorporating additional knowledge about (changing) flood protection measures in Venice.

3 Methods

3.1 Study area and storm event of 12 November 2019

The old-town of Venice covers an area of about 6 km^2 and is pervaded by more than 100 canals of depths between 1 and 5 meters [40]. The old-town is located in the Venetian lagoon, which is the largest Mediterranean with an area of about 550 km^2. The lagoon is connected to the Northern Adriatic Sea via three inlets at Lido, Malamocco and Chioggia, see figure 2.

On 12 November 2019, the second highest storm surge ever recorded flooded the old-town of Venice and other parts of the Venetian lagoon. The maximum measured water level of 189 cm ZMPS inside the old-town at the tidal gauge station Punta della Salute at 12 November 2019 22:50 CET. Such an extreme value was determined by the sum of the astronomical tide, a strong Sirocco wind blowing over the Adriatic Sea, a local depression – and the associated wind perturbation and an anomalously high monthly mean sea level in the Adriatic Sea [41].

It is noteworthy that the secondary low pressure field was not forecasted properly which lead to an underestimation of the flood by about 40 cm [41]. Unlike a storm event that occurred in 2018 where an even higher tidal peak (156 cm ZMPS) coincided with low astronomical tides (-10 cm ZMPS), the extreme sea level of 12 November 2019 was the product of less extreme, thus less unlikely conditions [27], [42].

As a response to the unexpected extreme meteorological event of 12 November 2019, financial support to the affected parties was provided in two rounds: 1) limited amounts for immediate response (up to EUR 5,000 for residents and EUR 20,000 for non-residential entities (companies, NGOs,...)) and 2) support for more extensive flood damages. Residents and entities could apply for compensation for either one or both of above rounds. In total 7,644 eligible claims were issued inside the study area with a total volume of about EUR 56.2 million.

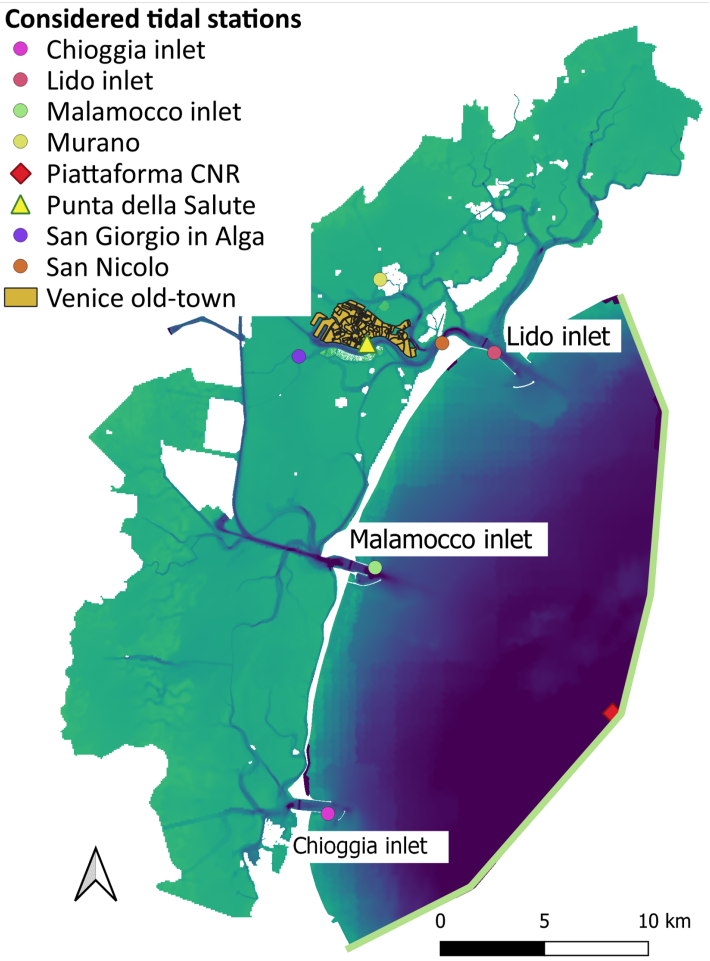

Figure 2: Study area consisting of part of the Adriatic shelf, the Venetian lagoon and the old-town of Venice. Green line indicates applied boundary condition for the water-level time-series.

For residents and entities which submitted only immediate response claims (total of 3,728 claims covering EUR 26.99 million of damages), the physical addresses of the claimants are publicly available. It was possible to allocate 95 % of the reported immediate response claims (EUR 25.73 million) to 2,778 structures inside Venice using a set of 33,096 addresses[2]. For claimants that submitted claims in both rounds or just for more extensive flood damages (EUR 29.21 million), information were provided on aggregated city-district level for data protection reasons[3].

3.2 SLR and MOSE scenarios

The developed framework is used applied to a set of different scenarios to derive indications of potential development of flood damage and flood risk in future. For this, a set of seven scenarios is used for the analysis. The scenarios differ in terms of mean sea level and closure behaviour of the MOSE barrier as summarized in table 1. For all scenarios, the meteorological forcing of a storm equivalent to the extreme event of 12 November 2019 is used.

[2]accessed here: `https://portale.comune.venezia.it/node/117/12181978`

[3]More information on and analysis of the available damage claim data can be found in the supplementary material of this study.

SLR0 considers a mean sea level as present in 2019. 'SLR0-allopen' represents the real flood event of 2019 without an operational MOSE barrier. Scenarios of 15 cm and and 45 cm sea level rise with respect to 2019 are selected in line with latest research on sea level rise prognosis in Venice: they correspond to the lower and upper confidence bounds of the projected sea level change in the Northern Adriatic Sea under RCP2.6 and RCP8.5 scenarios for the year 2060 respectively [43]. Regarding the MOSE barrier, two closure states are considered: a fully functioning MOSE barrier ('allclosed') and a set-up where all inlets but the Lido inlet close ('lidoopen'). The second closure state is chosen in line with previous studies indicating the prominent importance of the Lido inlet to manage water levels in Venice [35][44].

Table 1: Applied scenarios to assess future flood damages

	scenario	MSL [m]
present conditions	SLR0-allopen	0.34
	SLR0-allclosed	0.34
	SLR0-lidoopen	0.34
RCP 2.6 scenario	SLR1-allclosed	0.49
	SLR1-lidoopen	0.49
RCP 8.5 scenario	SLR2-allclosed	0.79
	SLR2-lidoopen	0.79

3.3 Hydrodynamic model

In the study area hydrodynamic models have been used frequently but without accounting for the urban area of Venice [45][46][47][48][49]. Studies looking into the distribution of flood depths in Venice have used a static model, also called bathtub model [50][4]. It uses the water level at the tidal gauge of Punta della Salute and compares it with the surface elevation of the old-town of Venice to identify the flood extent and depth.

For this study, a 2D hydrodynamic model based on Delft3D Flexible Mesh Suite 2021.04 was used [51]. The software provides a flexible unstructured grid framework which facilitates the grid generation in the complex coastal and urban setting [52]. Furthermore, it provides additional modules that could be used for a better physical representation of the system. In this study only 2D flow was considered but the model allows to account for additional processes like wave action or 1D flow of the sewage system[5].

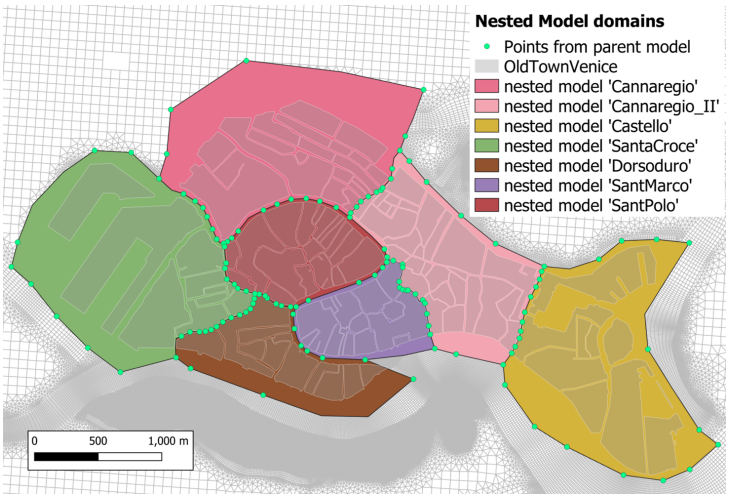

Figure 3: Nested model domains with observation points from parent model used as boundary forcing

An offline grid nesting framework was chosen consisting of a parent model covering the study area driving seven sub-models of higher resolution covering the area of the old-town of Venice. The parent model used 2.73 million elements covering the study area

[4]also mentioned here: `http://www.comune.venezia.it/maree`

[5]A more detailed reasoning along with additional information on the model set up are described in the supplementary material.

developed with an average grid resolution between 2.6 m in the old-town and 200 m at the Adriatic shelf. In the seven nested models grid resolution was increased to 1.3 m on average to reproduce the narrow street system in Venice. Water level time-series from the parent model simulation were extracted at 168 locations inside and around the old-town of Venice and used as inputs for the nested sub-models, as shown in figure 3. For every nested model, the maximum water level at each grid point was extracted. All grid points inside a 4m buffer around each structure were used to derive an average water level.

3.3.1 Model set-up

Most recent information on the depth of the lagoon flood plains, channels as well as the elevation of the islands of the old-town were accessed from various sources. Table 2 presents an overview of all used elevation data. All altimetry data were corrected to refer to ZMPS, the local chart datum in Venice.

Table 2: List of used altimetry data

altimetry data	datum	resolution	year	source
Venetian lagoon	IGM42 [6]	10m	2002	[53]
Tidal channels	ZMPS	0.50m	2013	[31]
Adriatic shelf	LAT [7]	550m	2018	[54]
old-town surface	IGM42	1m	2011	[55] [8]
Canals in old-town	IGM42	varying	2000	[56]

The parent model was forced by the time-series data of the tidal gauge station Piattaforma CNR (WGS84: $45.314242N$, $12.508314E$), which is located 15 km offshore in the Adriatic Sea. In addition, wind and pressure data from the Piattaforma CNR were used and applied uniform over the parent model domain. The used time-series data were corrected by a time shift of minus one hour to align with time series data used in other publications [57]. When considering climate change scenarios, a respective sea level rise was added to the time-series of the water level. The meteorological forcing was applied unaltered.

Constant standard values were used for the viscosity, diffusivity and density as flow in the Venetian lagoon is relatively well mixed without stratification [58]. Roughness was added as Manning-type n. A standard roughness value of 0.023 was applied to the entire study area and eventually altered in different areas of the model domain based on the predominant characteristics, as outlined in table 3. Roughness was used as a calibration factor. At the same time it was ensured that the values lie in the range of commonly applied roughness values for the different land types [59][15][60].

Table 3: Applied roughness values

area	n
tidal channels	0.025
tidal plains	0.040
northern lagoon	0.020
vegetation Venice	0.035
streets Venice	0.019
canals Venice	0.023
inlets	0.030

Similarly, the wind-induced shear stress by means of drag coefficient was used as a calibration parameter. It was implemented based on a linearly increasing relation between wind speed and wind drag developed by Smith & Banke [61]. However, as their relation

[6] 0 m IGM42 corresponds to + 0.23 m ZMPS

[7] When analyzing the water level time series of the Aqua Alta platform for different months of 2019, the LAT was chosen to correspond aproximately to $-0.40mZMPS$.

[8] The original altimetry data were collected by the RAMSES project (`www.ramses.it` which was conducted in the year 2011 as a topographic survey characterized by high precision (altimetric of 1 cm and planimetric of 2 cm). The used files have been made available by ArcGIS.

has been derived for wind speeds between 6 and 21 m/s, but extreme wind speeds for the 12 November 2019 reached up to 27 m/s, a higher drag coefficient of 0.00876 (for 100 m/s wind speed) was used. A comprehensive analysis of commonly used wind drag formulations confirmed that the chosen drag coefficient is within the range of available estimates [62]. In addition, it was confirmed that the chosen values are in line with other Delft3D-FM studies in the Venetian lagoon[9].

3.3.2 Modelling the closure of the MOSE barrier

The barrier system was modelled by means of a set of three simple weirs with a crest height defined by a time-series. It was assumed that the barrier crest height increases at constant speed from the bottom of the respective inlet up to a height of 3.00 m ZMPS and closes within 30 minutes [48]. For the considered meteorological storm conditions, the MOSE barrier starts closing when the tidal gauge station of Punta della Salute reaches a water level of 0.65 m [44]. This threshold was assumed to equal for all analysed scenarios. The starting time of closure was determined from modelled tidal gauge information from Punta della Salute for the different scenarios without a closing MOSE barrier, see table 4.

Table 4: Closure times for scenarios

Scenario	Closure time
SLR0	12/11/19 18:40
SLR1	12/11/19 18:10
SLR2	11/11/19 18:10

3.4 Damage Modelling

3.4.1 General approach for damage estimation

While general damage drivers are broadly acknowledged [63][64] the exact effect of hazard characteristics on an exposed structure is still poorly understood as it also heavily depends on the material and its quality [20][9]. This might be particularly true for cultural heritage sites built by special materials which quality have deteriorated by centuries of existence [21]. Consequently, the chosen model was selected with special care to allow for an inclusion of differing exposure and vulnerability characteristics.

Various approaches and post-flood data analysis have been conducted to develop relations between the flood hazard characteristics and corresponding tangible, direct damages. Several comparative studies have looked into the characterization and performance analysis of some frequently used damage models [65][66][67]. In general, loss estimates reflect high uncertainties and disparities because of the inaccuracy of the models and the lack of knowledge about the system in which they have been applied [66][6].

In this study, a flood model based on INSYDE (In-depth Synthetic Model for Flood Damage Estimation) was applied. It is a synthetic damage model developed based on 'what if' - scenario analysis to provide a methodical and generalized perspective on the flood-damage process for different building components individually [18]. It has been validated based on flood data from a river flood in Caldogno, Veneto, 2010. INSYDE is

[9]Personal communication G.Lemos, 24.05.2021

a multi-parametric model adopting 23 parameters to describe hazard, exposure and vulnerability characteristics of buildings[10]. As the model explicitly considers many damage mediating factors, it allows for direct adjustments or extensions of the model based on the available knowledge or considered research purposes [6][18][65]. As such, it is ideal to be extended to include new building types, e.g. heritage structures like churches etc., with specific hazard-structure responses. The INSYDE model also makes use of categorization into building types to account for differences in the exposure or vulnerability characteristics between typical buildings in a study area. As a result, the absolute damage D per structure is calculated as the sum of a set of damage components summarized in table 5:

$$D = \sum_{i=1}^{n}\sum_{j=1}^{m} C_{i,j} = \sum_{i=1}^{n}\sum_{j=1}^{m} up_{i,j} * ext_{i,j} * E[R] \quad (1)$$

where j represents the damage component and i describes the considered activity, e.g. cleaning, removal, and replacing. $Up_{i,j}$ is the unit price per damage component for for a given activity, $ext_{i,j}$ is the extent of exposed component and $E[R]$ the (expected) damage ratio. $E[R] \sim [0, 1]$ is derived from fragility functions for different hazard characteristics with gradual influence on the damage. They have been developed based on expert knowledge but are transparently reported as part of the supplementary material of Dottori et al. [18].

Table 5: Damage components considered in INSYDE. Red: not taken into account in this study.

	sub-component		sub-component
Clean-up	C1 – Pumping	Structural	S1 – Soil consolidation
	C2 – Waste disposal		S2 – Local repair
	C3 – Cleaning		S3 – Pillar repair
	C4 – Dehumidification		
Removal	R1 – Screed	Finishing	F1 – External plaster replacement
	R2 – Pavement		F2 – Internal plaster replacement
	R3 – Skirting		F3 – External painting
	R4 – Partition walls		F4 – Internal painting
	R5 – Plasterboard		F5 – Pavement replacement
	R6 – External plaster		F6 – Skirting replacement
	R7 – Internal plaster	Windows & Doors	W1 – Door replacements
	R8 – Doors		W2 – Window replacements
	R9 – Windows		
	R10 – Boiler		
Non-structural	N1 – Partition replacements	Building systems	P1 – Boiler replacement
	N2 – Screed replacement		P2 – Radiator painting
	N3 – Plasterboard replacement		P3 – Underfl. heating replacement
			P4 – Electrical system replacement
			P5 – Plumbing system replacement

These fragility functions follow truncated normal distributions and relate a probability of damage of a specific component to one flood hazard characteristic: flood depth, flood velocity or flood duration. In the present study, flood depth is the only damage mediating factor since flow velocity and flood duration were found to be too low to add an additional source of damage [18][68][11]. The fragility functions allow not only for a deterministic multi-parametric consideration of the flood-structure interaction but also to account for uncertainties in the flood-structure interaction in a probabilistic frame-

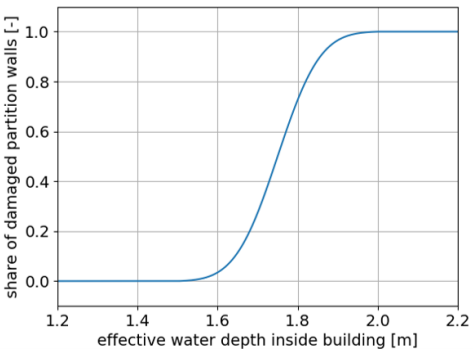

Figure 4: Fragility function for partition walls relative to water depth

[10]More details regarding the background and set up of the INSYDE model is provided in the supplementary material of this study.

[11]Results of the hydrodynamic model suggest that flood velocities are generally lower than 0.3 m/s and the flood duration is between 2 and 4 hours.

work. An example is shown in figure 4: damage to partition walls occurs if the partition walls absorbs too much water to be dried up, i.a. if water depth exceeds a certain threshold [18]. The fragility function can be used to determine an expected damage ratio or expected share of damaged partition wall for a given flood depth. However, damage to partition walls due to a certain water depth could range from 'no damage' to 'full damage' i.a. depending on the quality of wall (material). In the probabilistic framework, a large set of realizations for each component is drawn to derive the 5- and 95-percentiles expressing an optimistic and pessimistic estimate of the absolute damages. Even though the probabilistic framework was not used in this study, it might be useful in case of extending the framework to explicitly cover cultural heritage in Venice which might be more sensitive to varying flood characteristics.

3.4.2 INSYDE model set up

Information on the individual building area and extent were derived from cadastral data of the city of Venice [69]. In total 14,460 structures were considered. Information on the structural properties, the year of construction and the maintenance level were accessed from census data from year 2011 by the Italian National Institute of Statistics [70]. The census data provide information not building-specific but aggregated in census blocks covering multiple buildings. As a consequence, the most frequent characteristic was applied to all buildings within a census block[12].

GoogleMaps StreetView was used to gather visual information about typical house fronts, size and number of windows along with information about possible elevations of the entrance at ten random locations in different districts of the old-town. Moreover, advertisements by real estate agencies were used to characterise the interior of housings on the ground-floor in the old-town of Venice. They were used to estimate the average minimum height of electrical sockets, type of floor cover, presence of water-proof skirting boards and other protection measures. In addition, graphic documentation of the 12 November 2019 storm surge by the Aqua Grande project[13] was used to search for installed flood protection measures.

It was found that typical characteristics of residential buildings do not differ significantly from the implemented characteristics in INSYDE. One major difference related to the external wall perimeter exposed to floods was detected and incorporated as a new parameter EP_{eff}: most buildings in Venice are attached to other buildings reducing the exposed perimeter. Additionally, a new building type 'buildings with economic activities on the ground floor' (BEA) was added to account for observed differences in the exposure and vulnerability characteristics from typical residential buildings: the windows are generally larger (increased from 1.4m x 1.4m to 2m x 2m), the window sills are lower (new sill height of 0.5m instead of 1.2m) and many shops are on ground level without any steps of elevation. Additionally, the internal perimeter (reduced from 2.5 to 1.5 time the external perimeter) and number of doors is smaller (reduced to 3 per 100 sqm).

[12]More detailed information on the census block data can be found in the supplementary material of this study.

[13]accessed from: `https://www.aquagrandainvenice.it/en/welcome`

It was detected that many buildings had installed mobile protection systems, mainly bulkhead protections, at doors and windows to protect the interior from flooding during the 12 November 2019 storm event. Other protection measures were not commonly installed and therefore not incorporated in the damage model. A new parameter $BuHe$, representing the bulkhead protection height was implemented to mediate the water level inside the buildings. Due to lack of data on the spatial distribution and protection height of mobile protection systems, three conceptual individual protection scenarios (IPS) were characterized and applied: expected IPS, risk averse IPS and risk-taking IPS. For the risk taking IPS, it was assumed that no bulkhead protection was installed at all. For the expected IPS, it was assumed that residents would install bulkheads protecting their building against the forecasted maximum water level (FC) at Punta della Salute incremented by a safety margin of 10 cm. For a risk averse IPS, the protection height also refers to the forecasted maximum water level at Punta della Salute but is incremented by a safety margin of 50 cm. The water level h inside the buildings is consequently calculated as

$$h = h_e - GL - BuHe \quad \text{and} \quad BuHe = \begin{cases} 0 & \text{, if risk-taking IPS} \\ FC + 0.1 & \text{, if expected IPS} \\ FC + 0.5 & \text{, if risk averse IPS} \end{cases} \tag{2}$$

where h_e is the water level outside the buildings, GL is the ground floor level of the considered structure and $BuHe$ is the bulkhead protection height as visualized in figure 5. FC was set to 150 cm ZMPS for 'SLR0-allopen' and to 110 cm ZMPS in all other scenarios given that a functional MOSE barrier is expected to keep the water level below a threshold of 110cm ZMPS.

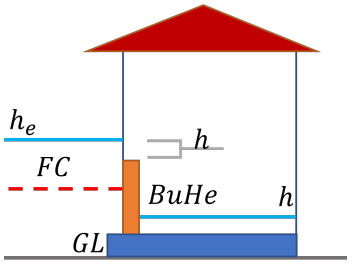

Figure 5: Visualization of bulkhead protection height

As a third parameter, information on the cultural heritage status of buildings[14] inside Venice was used to account for higher reconstruction costs. In line with a previous study assuming cost increase of reconstruction for artistic buildings by 7 to 11 % [38], total damage costs were incremented by 10 % in case of cultural heritage status. This is also in line with commonly mentioned ranges of reconstruction costs in Venice [71]. Unit prices for cleaning, removal and replacement were used from the INSYDE model assuming that those values do not significantly vary across Italy. INSYDE provides prices at 2015 price level. They were corrected for inflation and referenced to the year 2019.

4 Results

This study developed a methodical framework to assess present and future flood risk in the historic city of Venice. As such, a hydrodynamic model was developed, calibrated and validated. In addition, a damage model was transferred and compared against available

[14]Provided by the cultural heritage office of the city of Venice.

damage claim data of the storm event of 12 November 2019. Ultimately, the framework was applied to analyse development of future flood damages under sea level rise scenarios in case of a (partially) closing MOSE barrier.

4.1 Calibration & validation of the hydrodynamic model

For calibration and validation of the hydrodynamic parent model, modelled water levels were compared against measurements obtained at seven tidal gauge stations: Lido inlet, Malamocco inlet, Chioggia inlet and San Nicolo, Murano, San Giorgia in Alga and Punta della Salute which are located in close proximity to the old-town, as visualized in figure 2. Water level information were provided by the meteo-tidal network of the Venice Lagoon[15].

Three events were used for calibration and validation purposes as shown in table 6. For the tide calibration, a summer period was chosen where influence of wind on the water levels inside the lagoon can be expected to be low. The full model was calibrated for the storm event of 12 November 2019 and finally validated for another storm event from October 2018.

Table 6: Considered conditions for calibration and validation

used for	period
tide calibration	01/07/13 00:00 - 04/07/13 23:50
wind calibration	12/11/19 00:00 - 13/11/19 02:00
model validation	28/10/18 16:00 - 30/10/18 02:00

To evaluate the performance of the model, the Pearson R coefficient and the Root-Mean-Square-Error were used. Results for the three runs are compiled in table 7 and suggest that measured data can be reproduced well, including the storm surge peaks for the wind calibration and validation run. Accuracy of the maximum flood peak lies within a margin of $\pm 5cm$. For San Nicolo, Malamocco and Murano, the observed water level data were partly corrupted or not available.[16].

Table 7: Parent model performance

	tide calibration		wind calibration		model validation	
station	R	RMSE [m]	R	RMSE [m]	R	RMSE [m]
Murano	0.969	0.048	-	-	0.992	0.078
PuntaSalute	0.977	0.043	0.987	0.078	0.990	0.068
SanGiorgio	0.970	0.049	0.989	0.070	0.989	0.097
SanNicolo	0.989	0.027	0.945	0.136	-	-
Malamocco	0.971	0.054	0.984	0.081	-	-
Chioggia	0.993	0.025	0.977	0.091	0.934	0.114
Lido	0.986	0.040	0.974	0.097	0.945	0.121

The nested models were used to derive the flood depth estimates inside the city. Analysis of the difference in water depth estimates inside the old-town of Venice from the parent and nested model domains suggest that the grid resolution of the hydrodynamic model has significant impact on the flood characteristics inside the city. As figure 6b shows, a coarser grid tends to provide lower flood depth estimates. A coarser grid might fail (more often) to resolve possible flow paths in the very narrow street-system in Venice limiting water flow into the old-town.

Inside the old-town, a lack of available measured data did not allow for calibration. Instead, a cross-model comparison of the nested model flood depth estimates with a

[15]accessed here: `https://www.venezia.isprambiente.it/rete-meteo-mareografica`

[16]Further analysis of the results can be found in the supplementary material of this study.

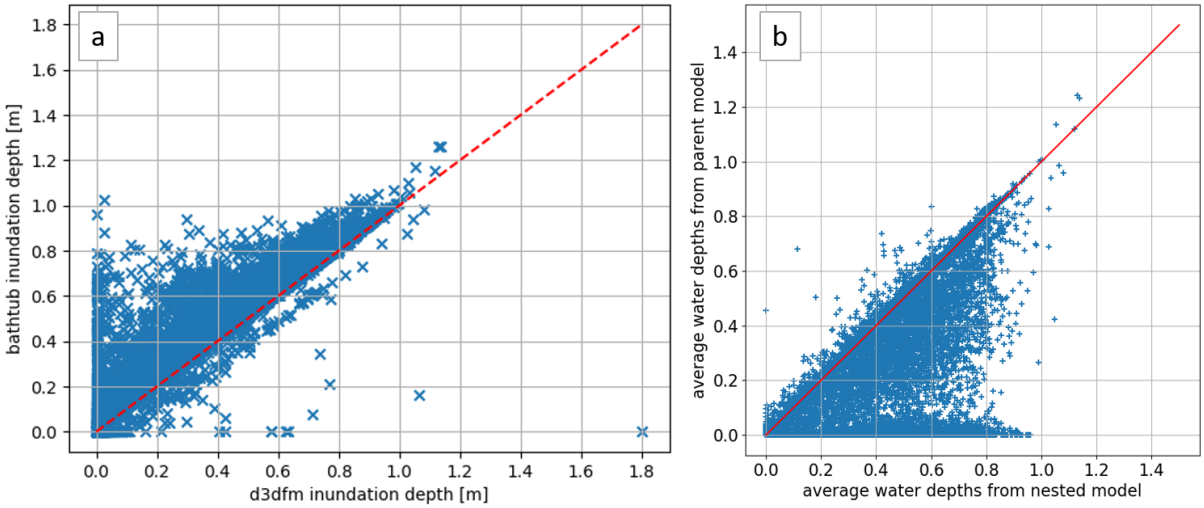

Figure 6: Flood depth estimates for old-town of Venice. a: Cross-model comparison of average inundation depths. b: Comparison of average flood depths (except Castello) for a grid resolution of 2.6m (parent model) and 1.3m (nested models).

simple bathtub model was used to analyse the average maximum flood depth estimates for the 12 November 2019 storm event. The bathtub model tends to provide higher inundation estimates as figure 6 shows. Additionally, it is visible that the hydrodynamic model gives high flood depths for some buildings while the bathtub models suggests that those structures are not affected by water levels at all (or to a much lesser degree). This unexpected result was linked to grid instabilities of the nested models. In total, higher water levels were suggested by the hydrodynamic model at 383 buildings. Additionally, grid instabilities of the nested sub-model 'Castello' (refer to figure 3) could not be resolved, resulting in missing flood depth data based on the hydrodynamic model for 2,098 buildings (14 % of the total number of buildings). For buildings affected by instabilities, flood depth estimates from the bathtub model were used for the damage modelling of these buildings.

4.2 Damage model performance

To analyse the performance of the transferred model, the total modelled damages for the old-town were compared against the total sum of the eligible 7,644 damage claims. Additionally, a structure-wise analysis was conducted for the sub-set of 2,778 structures with 3,728 immediate response claims.

Table 8: Comparison of damage estimates and claims [EUR million]

		INSYDE	claims
sub-set of structures	risk averse IPS	12.9	25.7
	expected IPS	42.0	
	risk taking IPS	63.1	
all structures	risk averse IPS	52.3	56.2
	expected IPS	166.3	
	risk taking IPS	253.6	

As shown in table 8, the damage model is able to reproduce the damage claims well: for both sets of considered structures, reported damage claims fall inside the range of modelled damage estimates for the different IPS. While the total volume of reported immediate response claims corresponds to a individual protection scenario between 'risk averse' and 'expected', the total volume of all reported damages is closer aligned with a risk averse IPS.

Additionally, a structure-wise comparison was conducted for 2,778 structures. As shown in table 9, correlation as well as the average relative error, computed as the ratio of the reported damage and the estimated damage per building, suggest limited alignment of the modelled damages with the reported claims. Both indicators suggest that the damage claims might be slightly better estimated based on a expected IPS or risk taking IPS for the majority of buildings. At the same time the RMSE, which gives more weight to extreme variations due to its definition, is lower when assuming a risk averse IPS. Moreover, the Kernel density plot gives insight in the relative frequency of damages as shown in figure 7. It can be seen that in a risk averse IPS, the number of structures with rather low damages is overestimated, meanwhile larger damages are underestimated. The opposite applies to risk neutral and risk taking scenarios.

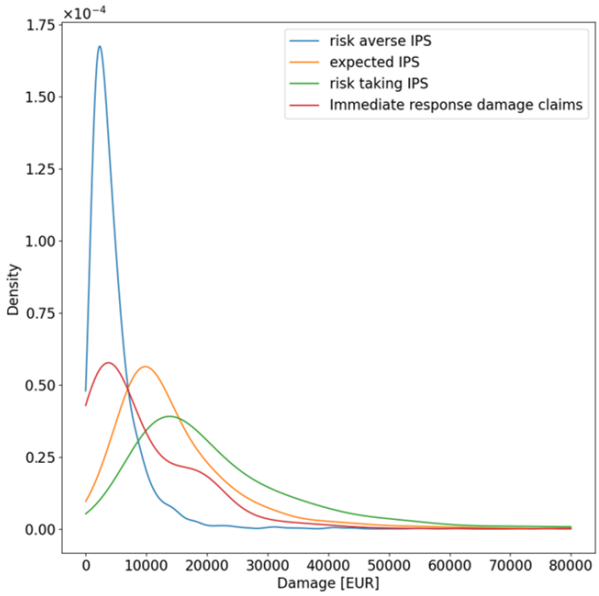

Figure 7: Kernel density plot: damage estimates and claims

According to the INSYDE model, the most affected building components are external and internal plaster removal (R6, R7), replacement (F1, F2) and painting (F3, F4), followed by costs for the replacement of electrical (P3) and plumbing systems (P4), as shown in figure 8. It can be seen that the model suggests no damage for many damage components as hazard characteristics are below thresholds for which damage is reported to occur. It can be seen that the expected IPS leads to limited damage reduction regarding plaster, but a strong reduction for the building systems. In a risk averse IPS, no damage occurs inside the buildings.

Table 9: Performance indicators for structures with immediate response claims

	risk averse IPS	expected IPS	risk taking IPS
R [-]	0.22	0.26	0.26
RMSE [EUR]	19,382	22,158	29,332
RE [%]	308.9	87.8	55.5

It is worth mentioning that damage estimates based on flood depth information from the bathtub model generally give similar damage estimates for both sets of considered structures; deviations for risk averse and risk taking IPS is between 1.5 and 6.3 %. For the expected IPS damages are about 13.1 to 16 % higher when using bathtub model depth estimates. This is a reasonable observation, given that the bathtub model generally provides higher flood depth estimates. As a result, the number of buildings where the flood depth exceeds the protection height according to bathtub model while the protection height can prevent flooding of structures according to the hydrodynamic model is higher for the expected IPS than for the risk taking or risk averse IPS. Consequently, more additional damage occurs according to the bathtub model for the expected IPS as significantly more buildings are damaged inside according to the bathtub model.

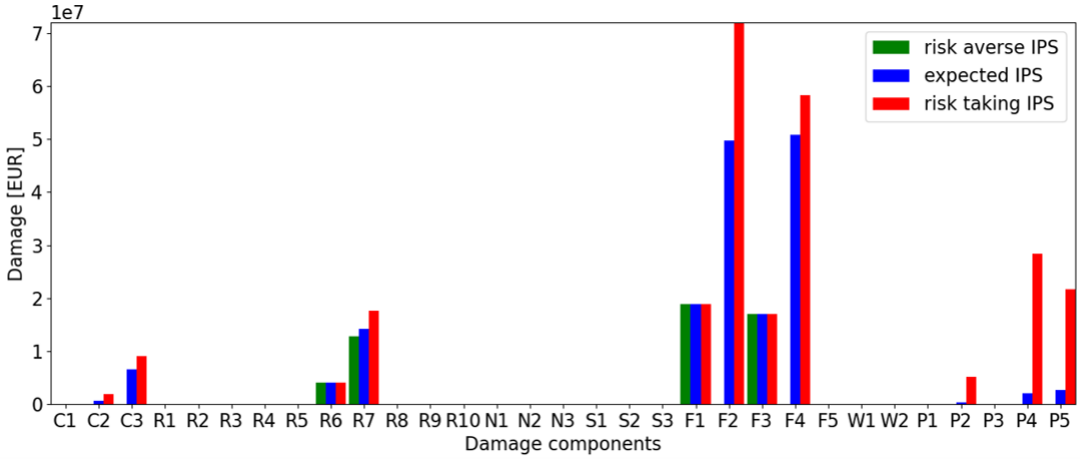

Figure 8: Damage components and damage estimation for all structures for SLR0-allopen

4.3 Flood damage for future scenarios

The developed flood risk assessment framework was applied to a set of sea level rise scenarios for the reference year of 2060. Flood damage was computed and used as a proxy of how flood damages and risk could evolve in future conditions. The set of seven scenarios is compiled in table 1. As shown in figure 9a, a fully closed MOSE barrier keeps the peak flood level significantly below the safety threshold of 110 cm ZMPS for the given meteorological event for all scenarios. A partially closed barrier would lead to a reduction of the flood peak in the order of 30 cm for SLR0 and SLR1. Still, an open Lido inlet leads to high water levels at Punta della Salute. Results suggest that the dampening effect by a partially closed barrier diminishes for SLR2: for a sea level rise of 45 cm, the peak at the Piattaforma CNR would be at 225 cm ZMPS, and the peak at Punta della Salute at 210 cm ZMPS implying that the damping effect is reduced by half.

It is noteworthy that for the 'allclosed' scenarios, SLR2 results in a slightly lower flood peak estimate than the other two scenarios. A possible explanation is that for SLR2 the closure of the MOSE barrier occurs about 24 hrs earlier relative to the flood peak while for SLR0 and SLR1 it is closed about 4 hrs before the flood peak. As the barrier is closing during flood, the part of the tidal wave that propagated into the lagoon before the full closure has more time to evenly spread out across the lagoon, resulting in a slightly lower average flood depth in the centre of the lagoon than for the other two scenarios. This ultimately influences the wind effect and maximum water levels at Punta della Salute.

Analysis of the implications of the different scenarios on the average inundation depths concludes that a partially functioning MOSE barrier would reduce the expected average flood depth for 90 % of the buildings significantly for sea level rise scenarios of SLR0 and SLR1 while in SLR2 the increased sea level dominates over the dampening effect of the partial closure as visualized in figure 9b. This analysis also shows that for the storm surge of 12 November 2019, 50 % of all structures in Venice experienced a flood depth of 55 cm or higher. Only 10 % of buildings experienced flood depths lower than 10 cm and only 5% of buildings were not exposed to floods at all.

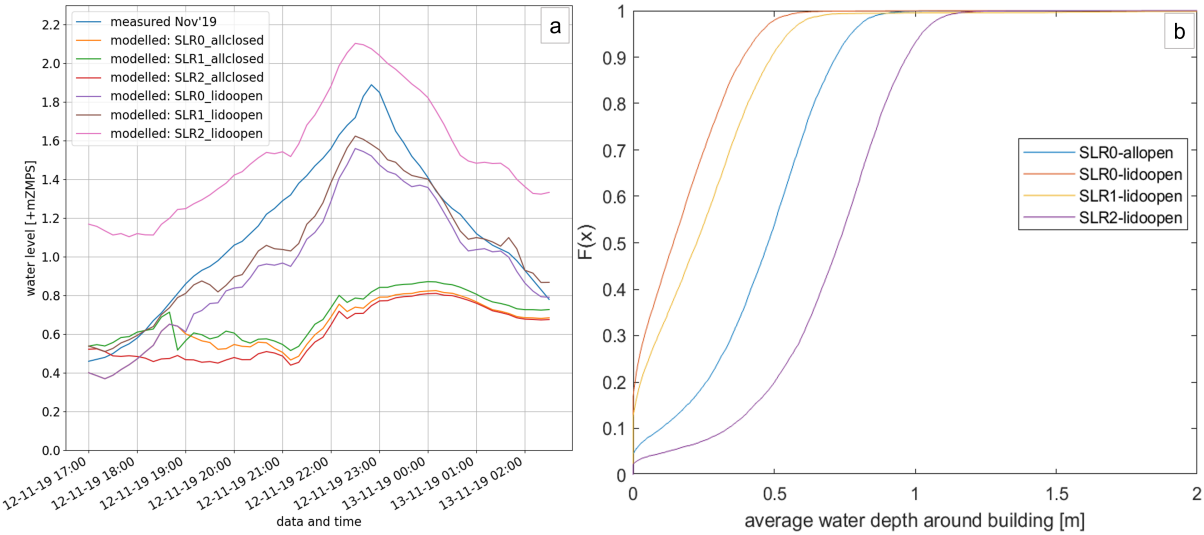

Figure 9: Flood depths for scnearios. a: Modelled flood peaks at Punta della Salute. b: Share of buildings exposed to certain average flood depths

Corresponding damage estimates for the different scenarios were computed using the calibrated INSYDE model. For the scenarios accounting for an (assumed) protecting MOSE barrier, the forecasting water level relevant to determine the height of mobile protections at doors and windows was set to the safety threshold of 110 cm ZMPS. As a result, the damage cost difference between expected IPS and risk averse IPS decreases with increasing flood depths. At the same time, the difference for the risk averse IPS is less apparent given that for SLR0-allopen, damages only occurred at the external walls, but for SLR0-lidoopen also partly on the inside due to lower protection levels. Results are compiled in table 10.

Table 10: Flood peak level at Punta della Salute [m ZMPS] and damage estimates [EUR million] for different scenarios

scenario	peak level	risk averse IPS	expected IPS	risk taking IPS
SLR0-allopen	1.89	52.2	166.3	253.6
SLR0-lidoopen	1.56	37.1	95.0	132.0
SLR0-allclosed	0.82	0.004	0.004	0.015
SLR1-lidoopen	1.62	42.6	129.4	166.7
SLR1-allclosed	0.87	0.006	0.006	0.02
SLR2-lidoopen	2.10	179.7	289.6	309.4
SLR2-allclosed	0.81	0.004	0.004	0.015

An interesting observation could be made when comparing the damage estimates of SLR0-allopen to those of SLR2-lidoopen. Despite an approximately 21 cm higher flood depth for SLR2-lidoopen, the effect on damage estimates for risk taking IPS and expected IPS are smaller than expected even though protection heights are on average also 40 cm lower than in SLR0-allopen. Analysis of the formulations for vulnerability and exposure implemented in INSYDE provide a possible explanation: not only the part of external and internal plaster in direct contact with the water has to be replaced, but also an additional height of one meter. Given that cost for plaster removal is independent of the required removal height, this implies that for a small flood depth, higher replacement costs occur already which are only incremented linearly for higher flood depths. As extreme flood depths are frequently lower than one meter, the influence of the additional height weights heavy compared to the difference for higher water level scenarios.

5 Discussion

Venice is a city with a long lasting history of flooding that is likely to extend into future despite the presence of the MOSE barrier. Until now, limited methodical approaches were available to provide estimations of future flood risk to structures and particularly to cultural heritage. As a consequence, this study developed a flood risk assessment framework that can be used for assessment of direct, tangible damages to residential and economic buildings, but could be extended in future research to account for the special conditions of cultural heritage as well. The framework performs well compared to available damage claim data and gives some indications about possible future flood risk for extreme storm surges under a partially failing MOSE barrier system.

The developed hydrodynamic model provides reliable estimates of hazard characteristics inside the old-town. Firstly, the validated hydrodynamic coastal model reproduces the flood peaks with an accuracy of $\pm 5cm$. Simplifications of the lagoon system such as applying uniform meteorological conditions over the entire domain and neglecting freshwater inputs and wave action had no significant negative effect on the performance of the model. Secondly, the cross-model comparison suggests that the hydrodynamic model performs as expected and might rather provide optimistic flood depth estimates inside the city compared to the presently used static model [72]. A final confirmation of the flood depths inside the city by means of calibration and validation flood depth records was not possible but should be a key focus in future studies as flood-enhancing components such as the sewage system, water coming from the ground or wave influence were neglected. In addition, following from the comparison of parent and nested model depth estimates, a grid convergence analysis should be conducted to find the optimal grid resolution for the city of Venice: despite a grid resolution of 1.3m near structures that is already rather high compared to other hydrodynamic urban models [15], the specific setting of Venice with its narrow street system might require to increase the resolution even further.

Some modelling challenges of the hydrodynamic model have to be highlighted. Because of the complex urban structures and altimetry, some extreme local water levels occurred in the parent and nested models likely caused by the complex grid structure and the algorithm describing the wetting and drying process inside the model [51]. This led not only to incorrectly high flood depths at a few buildings but also prevented the consideration of one of the nested sub-models. Part of the instabilities could be solved by grid refinement, bathymetry alteration or adjusting the modelled time periods. In accordance to previous studies [73][6] it was found acceptable to use bathtub flood depth estimates for the remaining structures instead, given the limited influence of flood depth variation on the damage estimate. At the same time it has to be highlighted that an fully functioning hydrodynamic model might add additional benefits to the flood risk assessment framework as it can account for (changing) physical characteristics explicitly, allows for a proper calibration and could also incorporate additional flow path-components such as a 1D sewage system.

The adjusted version of the INSYDE damage model is able to reproduce the total damage claim volume related to the storm event of 12 November 2019 as shown in table 8. Analysis for the sub-set of immediate response damage claims also confirm initial ex-

pectations of relatively high individual protections levels in Venice as frequent and intense experience of flooding have been reported to contribute to higher levels of individual flood preparedness [74]. Moreover, results imply that the effect of protection measures has a strong influence on the estimated damages.

However, the poor structure-wise correlation as well as the alignment of the two considered sets of reported damage claims with different (combinations) of IPS reiterate commonly faced challenges of flood damage modelling [59]. Limited knowledge about the system introduces uncertainty in the damage estimates. As an example, about half of all damage claims (total of 7,644) were linked to about 20 % of the structures in Venice only, meanwhile 90 % of structures were found to be exposed to an average flood depth of at least 0.1 m according to the hydrodynamic model. Thus, it is questionable whether exposure and vulnerability of the system are adequately represented given that modelled damages of external walls alone are almost as high as the reported damages. In addition, preparedness was simplified as perfectly functioning mobile barrier systems installed at all buildings likewise in this study, meanwhile protection levels have been reported to be very diverse[17] and could also (partially) fail to provide the promised level of protection in reality. Additionally, more protection measures could be in place that reduces the flood damages. Moreover, many exposure and vulnerability relations of the synthetic damage model were transferred unaltered despite the possibility that they might not reproduce the present hazard-structure interaction processes in Venice.

At the same time, limitations of the the available damage claim data-sets have to be accounted for as well. It can generally be questioned whether reported damages represent the full set of effective damages of a flood event; potential claimants might have avoided to undergo significant bureaucratic efforts for (sometimes) limited financial support [65]. Alternatively, claimants might not have seen the need to replace (some) damaged elements, e.g. because of their experience with frequent flooding. Marks of previous floods at house fronts throughout the old-town support this hypothesis. Additionally, given that the available damage data are spatially and/or component-wise aggregated, limited conclusions can be drawn form the damage data analysis to address the mentioned limitations of the framework. Information from a detailed investigation of the effective and reported damages for the 12 November 2019 flood event might provide required additional confidence in the developed damage model. Also, a thorough analysis of the variety and spatial distribution of building types, installed preparation and protection measures on structure and neighborhood level as well as other exposure characteristics in Venice would be required for a better representation of the system.

When discussing the accuracy and reliability of the applied damage model it is also worth considering that another study analysing exceptionally extreme flood events suggests much higher flood damages [39]; for flood events exceeding 180 cm ZMPS, damage estimates amount for EUR 196.33 million[18] even though only the refurbishment (plastering) of walls is considered. Given the varying approaches, many reasons could contribute to the diverging damage estimates. Two striking reasons were identified: estimates about the buildings requiring special care due to their historical importance diverge for the two

[17] Personal communication, C. Ferrarin.

[18] Price level of 2013, not adjusted for inflation.

studies (present study: 25 % of buildings declared as cultural heritage, in other study 50 % of buildings) along with the corresponding increase in refurbishment cost (present study: 10%, other study 50%). Additionally, the assumed basis reconstruction costs might vary: in the present study reconstruction cost values from another region were used under the assumption of limited variation across Italy. It would be recommended to investigate possible differences and use reconstruction cost information for the Veneto region instead if necessary[19].

Results on the effect of the MOSE barrier on the water level inside the lagoon align with previous studies suggesting that a partial closure will still cause flooding of the old-town of Venice [48]. The study adds to the existing knowledge as it considers the second most extreme flood event experienced while previous studies have mainly investigated more frequent, less extreme flood events [44][75]. The present study adds new insights suggesting that the damping effect of a partially closed MOSE barrier on the flood wave will reduce for increasing sea level rise and might consequently amplify flood risk in future. To confirm this finding in future studies, some of the present's study limitations should be addressed: for the applied future scenarios, present conditions of the system were used. However, the sediment budget of the lagoon is negative, meaning that the lagoon currently deepens and might look significantly different in 40 years from now [76]. Same applies for local subsidence processes which have contributed to flood risk in the past significantly and might do so in future as well [43]. Also, variation in tidal amplitude due to changes in bathymetry and mean sea level as observed in the past, might continue in future as well [49].

In addition, it has to be mentioned that some inaccuracy regarding the flood levels is likely to be introduced as processes of seepage through the barrier along with freshwater input in the lagoon have been neglected in the present study. This could be particularly relevant for SLR2, where the MOSE barrier would be closed for more than 36 hours. In previous studies it has been suggested that seepage through the fully closed barrier could result in water level increase between 2.7 to 21 mm per hour [35]. Consequently, peak water level could be expected to be about 8.1 to 63 cm higher for SLR2-allclosed, while the effect of seepage could add between 1 and 8.4 cm in a SLR0-allclosed scenario where MOSE closure happens about 4 hours before the flood peak. Seepage and freshwater input might also increase water levels for scenarios with an open inlet at Lido.

The results of the scenario analysis highlight the importance of a fully functioning MOSE barrier and the damage mediating influence of the individual protection scenarios. In line with previous studies investigating the remaining flood risk under climate change with a fully functioning barrier [37], the present study suggests that a fully closed MOSE barrier limits the effect of flooding for the considered meteorological flood event to very few buildings inside the old-town with very small damages for all considered sea level rise scenarios as shown in table 10.

Even though the applied methodology to represent preparedness and individual flood risk protection by means of different IPS and their effectiveness has mainly a conceptual

[19]accessible here: `https://www.regione.veneto.it/web/lavori-pubblici/prezzario-regionale`

value, some insights can be derived nevertheless: the warning level and how residents will respond to this in terms of individual protection in light of a (expected) functioning MOSE barrier appear to have significant influence on the expected damages as shown in table 11. Table 11 visualizes the change of estimated damage for the different scenarios referenced to the modelled damages for the flood event of 12 November 2019 represented by SLR0-allopen. It can be seen that a partially functioning MOSE barrier could reduce damages of a storm surge event like 12 November 2019 by 17 % to 48 % for SLR0 or SLR1 under the assumption of unaltered level of individual protection levels in future; the reduction is strongest for SLR0-lidoopen under assumption of a (constant) risk-taking IPS, where damage would be reduced to 52 % of damages estimated for SLR0-allopen. As discussed, the damping effect of a partially closed barrier diminishes for SLR2-lidoopen. As a result, damages could increase by a factor 1.22 to 3.44 if sea level rise follows the pessimistic prognosis of climate change.

Table 11: Ratio of future flood damages and SLR0-allopen under varying IPS (developments in future). I: risk averse IPS, II: expected IPS, III: risk taking IPS.

		SLR0_lidoopen			SLR1_lidoopen			SLR2_lidoopen		
		I	II	III	I	II	III	I	II	III
SLR0 allopen	I	0.71	1.82	2.53	0.82	2.47	3.19	3.44	5.54	5.92
	II	0.22	0.57	0.79	0.26	0.78	1.00	1.08	1.74	1.86
	III	0.15	0.37	0.52	0.17	0.51	0.66	0.71	1.14	1.22

At the same time, individual protection levels might change in future depending on the performance and reliability of the MOSE barrier. In the worst case, meaning that protection levels change from a risk averse IPS to a risk taking IPS, damages could be up to 5.92 times higher compared to flood damages of SLR0-allopen as shown in table 11. Compared to a scenario where the individual protection level remains constant, damages would be about 72 % higher in this case as shown in Tab. 10. At the same time, in case that individual protection levels increase from an expected IPS to a risk averse IPS, damages could be reduced to 26% for SLR1-lidoopen or just slightly increase by 8 % in case of SLR2-lidoopen.

As present knowledge on influencing drivers of future flood risk is very limited, this study can only be a starting point for a more concise analysis of the implications of the MOSE barrier on the old-town of Venice and the individual protection levels in particular. At this point it is unknown, what effect the operational MOSE barrier will have on the early-warning system in Venice and the level (and types) of installed protection measures by residents. Additionally, provided estimates are all based on present monetary values as well as on present exposure and preparedness conditions. They are expected to change in future, again not only depending on possible socio-economic and political developments but also depending on the reliability of the MOSE barrier to protect the old-town and its residents in the future.

6 Conclusion

In this study, a flood risk assessment framework has been developed. It was able reproduce the flood event of 12 November 2019 with an accuracy of $\pm 5cm$ in the proximity of

the old-town and provides damage estimates in accordance with available damage claim data. Limitations of the hydrodynamic model caused by local instabilities could be overcome by using information from a static model. The implemented damage model can reproduce damage claim data but faces commonly acknowledged uncertainties due to limited knowledge about the system and damage processes.

Developing a methodical risk assessment framework for the cultural heritage city has provided some valuable insights into expected flood exposure and damages in the old-town of Venice. While this study confirms the general appropriateness of the MOSE barrier to protect the city of Venice for extreme storm events for additional rising sea level up to 45 cm, it was also found that the damages in case of a partially closed MOSE barrier might still increase significantly for most considered scenarios: while an improved individual protection level in future could lead to a damage reduction of up to 78% for present sea level and 74 % for an optimistic sea level rise prognosis, damages could be up to 1.22 to 5.92 times higher in 2060 in case of unchanged or decreased level of individual protection. Based on the findings of relative importance of individual flood protection in light of a potentially failing MOSE barrier, this study provides indication that a better understanding of presently applied flood protection is needed to identify realistic individual protection scenarios for future conditions. This would be helpful to identify possible areas of action to maintain (or advance) existing structure-wise flood protections and individual preparedness. In addition, the influence of the MOSE barrier on the reported warning levels and the effectively installed protections was identified as an important question to address in order to reduce flood risk in Venice until 2060. As such, the proposed flood risk assessment framework provides a methodical approach useful to support future decisions on flood risk management.

Additional studies should be done to improve the presented framework. Addressing some of the limitations, particularly the simplification of the system by excluding the sewage system, grid instabilities and lack of calibration data might add additional confidence to the exposure modelling. Moreover, incorporating information on future return levels of storm events as well as failure probabilities of the MOSE barrier should be addressed and incorporated in the present framework to allow for a proper flood risk assessment to support the efficient and effective allocation of (additional) resources to flood protection in Venice. At the same time, a better understanding of the spatial distribution of protection measures and other exposure mediating characteristics within the districts of the old-town as well as on the level of structures would be required for a better representation of the system. Additionally, new building types in the damage model could be implemented to account for some characteristic cultural heritage buildings as proposed in the supplementary material. This would contribute to a better and multidimensional understanding of the present and future flood risk.

7 Acknowledgement

First of all, I would like to thank the members of my assessment committee; Prof. dr. ir. S.N. Jonkman for his outstanding amount of detailed feedback provided at the different

stages of this work as well as sharing contacts to experts for advanced discussions, Dr. ir. M.A. Diaz Loaiza for his frequent and constructive feedback on the work process, development of this paper and encountered challenges along the way, Dr. ir. C. Ferrarin for providing feedback, data required for the hazard modelling and insight in the general setting of the old-town of Venice, Dr. ir. A. Antonini for his commitment, scientific guidance on developing this paper and support in communication with Italian authorities, Dr. S. Fatorić, for her continuing support and extensive feedback on cultural heritage. Furthermore, I would like to issue special thanks to Dr. ir. A. R. Scorzini for her immediate support and sharing insights and experience from the complex field of damage modelling in the context of Italy, M. Calligaro for his valuable and cumbersome effort to provide all possible damage claim information, and G. T. M. Lemos for sharing insights of her experience on D3DFM modelling of the Venetian lagoon. In addition, I would like to thank the office of the delegated Commissioner Delegate for the Emergency resulting from the exceptional tide of November 12, 2019 in Venice, for their willingness and cooperation in providing statistical data related to the declared damages.

References

[1] M. I. Vousdoukas, L. Mentaschi, J. Hinkel, P. J. Ward, I. Mongelli, J.-C. Ciscar, and L. Feyen, "Economic motivation for raising coastal flood defenses in europe," *Nature Communications*, vol. 11, no. 1, p. 2119, 2020, ISSN: 2041-1723. DOI: 10.1038/s41467-020-15665-3. [Online]. Available: https://www.nature.com/articles/s41467-020-15665-3.

[2] J. Hinkel, D. Lincke, A. T. Vafeidis, M. Perrette, R. J. Nicholls, R. S. J. Tol, B. Marzeion, X. Fettweis, C. Ionescu, and A. Levermann, "Coastal flood damage and adaptation costs under 21st century sea-level rise," *Proceedings of the National Academy of Sciences*, vol. 111, no. 9, pp. 3292–3297, 2014, ISSN: 1091-6490. DOI: 10.1073/pnas.1222469111. [Online]. Available: https://www.pnas.org/content/111/9/3292.

[3] European Commission, *Eur-lex - 32007l0060 - en - eur-lex*, 5/18/2021. [Online]. Available: https://eur-lex.europa.eu/eli/dir/2007/60/oj (visited on).

[4] C. B. Field, V. Barros, T. F. Stocker, and Q. Dahe, Eds., *Managing the Risks of Extreme Events and Disasters to Advance Climate Change Adaptation: Special Report of the Intergovernmental Panel on Climate Change*. Cambridge: Cambridge University Press, 2012, ISBN: 9781139177245. DOI: 10.1017/CBO9781139177245.

[5] C. Arrighi, M. Brugioni, F. Castelli, S. Franceschini, and B. Mazzanti, "Flood risk assessment in art cities: The exemplary case of florence (italy)," *Journal of Flood Risk Management*, vol. 11, S616–S631, 2018, ISSN: 1753-318X. DOI: 10.1111/jfr3.12226.

[6] A. R. Scorzini and E. Frank, "Flood damage curves: New insights from the 2010 flood in veneto, italy," *Journal of Flood Risk Management*, vol. 10, no. 3, pp. 381–392, 2017, ISSN: 1753-318X. DOI: 10.1111/jfr3.12163.

[7] M. Amadio, J. Mysiak, L. Carrera, and E. Koks, "Improving flood damage assessment models in italy," *Natural Hazards*, vol. 82, no. 3, pp. 2075–2088, 2016, ISSN: 1573-0840. DOI: 10.1007/s11069-016-2286-0.

[8] Annegret H. Thieken, Klaus Piroth, Jochen Schwarz, Reimund Schwarze, and Meike Müller, "Methods for the evaluation of direct and indirect flood losses," in *4th International Symposium on Flood Defence:4th International Symposium on Flood Defence:Managing Flood Risk, Reliability and Vulnerability*. [Online]. Available: https://www.researchgate.net/publication/259273112_Methods_for_the_evaluation_of_direct_and_indirect_flood_losses.

[9] B. Merz and A. H. Thieken, "Flood risk curves and uncertainty bounds," *Natural Hazards*, vol. 51, no. 3, pp. 437–458, 2009, ISSN: 1573-0840. DOI: 10.1007/s11069-009-9452-6. [Online]. Available: https://www.researchgate.net/publication/227056811_Flood_risk_curves_and_uncertainty_bounds.

[10] D. Molinari and A. R. Scorzini, "On the influence of input data quality to flood damage estimation: The performance of the insyde model," *Water*, vol. 9, no. 9, p. 688, 2017. DOI: 10.3390/w9090688. [Online]. Available: https://www.mdpi.com/2073-4441/9/9/688.

[11] C. Arrighi, L. Rossi, E. Trasforini, R. Rudari, L. Ferraris, M. Brugioni, S. Franceschini, and F. Castelli, "Quantification of flood risk mitigation benefits: A building-scale damage assessment through the rasor platform," *Journal of environmental management*, vol. 207, pp. 92–104, 2018. DOI: 10.1016/j.jenvman.2017.11.017.

[12] J. Teng, A. J. Jakeman, J. Vaze, B. Croke, D. Dutta, and S. Kim, "Flood inundation modelling: A review of methods, recent advances and uncertainty analysis," *Environmental Modelling & Software*, vol. 90, pp. 201–216, 2017, ISSN: 1364-8152. DOI: 10.1016/j.envsoft.2017.01.006. [Online]. Available: http://www.sciencedirect.com/science/article/pii/S1364815216310040.

[13] J. Yin, S. Jonkman, N. Lin, D. Yu, J. Aerts, R. Wilby, M. Pan, E. Wood, J. Bricker, Q. Ke, Z. Zeng, Q. Zhao, J. Ge, and J. Wang, "Flood risks in sinking delta cities: Time for a reevaluation?" *Earth's Future*, vol. 8, no. 8, 2020, ISSN: 2328-4277. DOI: 10.1029/2020EF001614. [Online]. Available: https://agupubs.onlinelibrary.wiley.com/doi/full/10.1029/2020EF001614.

[14] H. A. Sai, T. Tabata, K. Hiramatsu, M. Harada, and N. C. Luong, "An optimal scenario for the emergency solution to protect hanoi capital from the red river floodwater using van coc lake," *Journal of Flood Risk Management*, 2020, ISSN: 1753-318X. DOI: 10.1111/jfr3.12661. [Online]. Available: https://onlinelibrary.wiley.com/doi/full/10.1111/jfr3.12661.

[15] Y. Xing, Q. Liang, G. Wang, X. Ming, and X. Xia, "City-scale hydrodynamic modelling of urban flash floods: The issues of scale and resolution," *Natural Hazards*, vol. 96, no. 1, pp. 473–496, 2019, ISSN: 1573-0840. DOI: 10.1007/s11069-018-3553-z.

[16] T. W. Gallien, B. F. Sanders, and R. E. Flick, "Urban coastal flood prediction: Integrating wave overtopping, flood defenses and drainage," *Coastal Engineering*, vol. 91, pp. 18–28, 2014, ISSN: 0378-3839. DOI: 10.1016/j.coastaleng.2014.04.007.

[17] E. Molinaroli, S. Guerzoni, and D. Suman, *Adaptations to Sea Level Rise: A Tale of Two Cities – Venice and Miami*. 2018. DOI: 10.31230/osf.io/73a25.

[18] F. Dottori, R. Figueiredo, M. L. V. Martina, D. Molinari, and A. R. Scorzini, "Insyde: A synthetic, probabilistic flood damage model based on explicit cost analysis," *Natural Hazards and Earth System Sciences*, vol. 16, no. 12, pp. 2577–2591, 2016, ISSN: 1561-8633. DOI: 10.5194/nhess-16-2577-2016. [Online]. Available: https://nhess.copernicus.org/articles/16/2577/2016/nhess-16-2577-2016.html.

[19] T. Tiggeloven, H. de Moel, H. C. Winsemius, D. Eilander, G. Erkens, E. Gebremedhin, A. Diaz Loaiza, S. Kuzma, T. Luo, C. Iceland, A. Bouwman, J. van Huijstee, W. Ligtvoet, and P. J. Ward, "Global-scale benefit–cost analysis of coastal flood adaptation to different flood risk drivers using structural measures," *Natural Hazards and Earth System Sciences*, vol. 20, no. 4, pp. 1025–1044, 2020, ISSN: 1561-8633. DOI: 10.5194/nhess-20-1025-2020. [Online]. Available: https://nhess.copernicus.org/articles/20/1025/2020/.

[20] Z. Huijbregts, J. W. M. van Schijndel, H. L. Schellen, and N. Blades, "Hygrothermal modelling of flooding events within historic buildings," *Journal of Building Physics*, vol. 38, no. 2, pp. 170–187, 2014, ISSN: 1744-2591. DOI: 10.1177/1744259114532613.

[21] M. F. Drdácký, "Flood damage to historic buildings and structures," *Journal of Performance of Constructed Facilities*, vol. 24, no. 5, pp. 439–445, 2010, ISSN: 0887-3828. DOI: 10.1061/(ASCE)CF.1943-5509.0000065.

[22] P. Hudson, W. W. Botzen, L. Feyen, and J. C. Aerts, "Incentivising flood risk adaptation through risk based insurance premiums: Trade-offs between affordability and risk reduction," *Ecological Economics*, vol. 125, pp. 1–13, 2016, ISSN: 0921-8009. DOI: 10.1016/j.ecolecon.2016.01.015. [Online]. Available: https://www.sciencedirect.com/science/article/pii/S0921800916301240.

[23] T. LÓPEZ-MARRERO, "An integrative approach to study and promote natural hazards adaptive capacity: A case study of two flood-prone communities in puerto rico," *Geographical Journal*, vol. 176, no. 2, pp. 150–163, 2010, ISSN: 1475-4959. DOI: 10.1111/j.1475-4959.2010.00353.x.

[24] H. Kreibich, I. Seifert, A. H. Thieken, E. Lindquist, K. Wagner, and B. Merz, "Recent changes in flood preparedness of private households and businesses in germany," *Regional Environmental Change*, vol. 11, no. 1, pp. 59–71, 2011, ISSN: 1436-378X. DOI: 10.1007/s10113-010-0119-3. [Online]. Available: https://link.springer.com/article/10.1007%2Fs10113-010-0119-3.

[25] D. Battistin and P. Canestrelli, *1872-2004: la serie storica delle maree a Venezia*. Instituzione Centro Previsioni e Segnalazioni Maree, 2006.

[26] P. Lionello, D. Barriopedro, C. Ferrarin, R. J. Nicholls, M. Orlic, F. Raicich, M. Reale, G. Umgiesser, M. Vousdoukas, and D. Zanchettin, "Extremes floods of venice: Characteristics, dynamics, past and future evolution," *Natural Hazards and Earth System Sciences Discussions*, pp. 1–34, 2020, ISSN: 1561-8633. DOI: 10.5194/nhess-2020-359. [Online]. Available: https://nhess.copernicus.org/preprints/nhess-2020-359/.

[27] S. Morucci, E. Coraci, F. Crosato, and M. Ferla, "Extreme events in venice and in the north adriatic sea: 28–29 october 2018," *Rendiconti Lincei. Scienze Fisiche e Naturali*, vol. 31, no. 1, pp. 113–122, 2020, ISSN: 1720-0776. DOI: 10.1007/s12210-020-00882-1.

[28] I. Međugorac, M. Pasarić, and I. Güttler, "Will the wind associated with the adriatic storm surges change in future climate?" *Theoretical and Applied Climatology*, pp. 1–18, 2020, ISSN: 1434-4483. DOI: 10.1007/s00704-020-03379-x. [Online]. Available: https://link.springer.com/article/10.1007/s00704-020-03379-x.

[29] P. Lionello, M. B. Galati, and E. Elvini, "Extreme storm surge and wind wave climate scenario simulations at the venetian littoral," *Physics and Chemistry of the Earth, Parts A/B/C*, vol. 40-41, pp. 86–92, 2012, ISSN: 14747065. DOI: 10.1016/j.pce.2010.04.001.

[30] G. Jordà, D. Gomis, and M. Marcos, "Comment on "storm surge frequency reduction in venice under climate change" by troccoli et al," *Climatic Change*, vol. 113, no. 3-4, pp. 1081–1087, 2012, ISSN: 1573-1480. DOI: 10.1007/s10584-011-0349-5.

[31] F. Madricardo, F. Foglini, A. Kruss, C. Ferrarin, N. M. Pizzeghello, C. Murri, M. Rossi, M. Bajo, D. Bellafiore, E. Campiani, S. Fogarin, V. Grande, L. Janowski, E. Keppel, E. Leidi, G. Lorenzetti, F. Maicu, V. Maselli, A. Mercorella, G. Montereale Gavazzi, T. Minuzzo, C. Pellegrini, A. Petrizzo, M. Prampolini, A. Remia, F. Rizzetto, M. Rovere, A. Sarretta, M. Sigovini, L. Sinapi, G. Umgiesser, and F. Trincardi, "High resolution multibeam and hydrodynamic datasets of tidal channels and inlets of the venice lagoon," *Scientific Data*, vol. 4, no. 1, p. 170 121, 2017, ISSN: 2052-4463. DOI: 10.1038/sdata.2017.121. [Online]. Available: https://www.nature.com/articles/sdata2017121?fref=gc&dti=211246695634785.

[32] U. W. H. Centre, *Venice and its lagoon*, 12/11/2020. [Online]. Available: https://whc.unesco.org/en/list/394/ (visited on).

[33] J.-J. Wang, "Flood risk maps to cultural heritage: Measures and process," *Journal of Cultural Heritage*, vol. 16, no. 2, pp. 210–220, 2015, ISSN: 12962074. DOI: 10.1016/j.culher.2014.03.002.

[34] Comune di Venezia., *Rischio idraulico*, 2016. [Online]. Available: https://www.comune.venezia.it/it/content/rischio-idraulico (visited on).

[35] G. Umgiesser and B. Matticchio, "Simulating the mobile barrier (mose) operation in the venice lagoon, italy: Global sea level rise and its implication for navigation," *Ocean Dynamics*, vol. 56, no. 3-4, pp. 320–332, 2006, ISSN: 1616-7228. DOI: 10.1007/s10236-006-0071-4.

[36] L. Cavallaro, C. Iuppa, and E. Foti, "Effect of partial use of venice flood barriers," *Journal of Marine Science and Engineering*, vol. 5, no. 4, p. 58, 2017. DOI: 10.3390/jmse5040058. [Online]. Available: https://www.mdpi.com/2077-1312/5/4/58/htm.

[37] Nunes, Paulo A. L. D., M. Breil, and G. Gambarelli, *Economic Valuation of on Site Material Damages of High Water on Economic Activities based in the City of Venice: Results from a Dose-Response-Expert-Based Valuation Approach*. 2005. DOI: 10.2139/ssrn.702965.

[38] F. Fontini, G. Umgiesser, and L. Vergano, "The role of ambiguity in the evaluation of the net benefits of the mose system in the venice lagoon," *"Marco Fanno" Working Papers*, no. 0080, 2008.

[39] M. Caporin and F. Fontini, *The Value of Protecting Venice from the Acqua Alta Phenomenon under Different Local Sea Level Rises*. 2014. [Online]. Available: https://mpra.ub.uni-muenchen.de/53779/.

[40] G. Umgiesser, M. Bajo, C. Ferrarin, A. Cucco, P. Lionello, D. Zanchettin, A. Papa, A. Tosoni, M. Ferla, E. Coraci, S. Morucci, F. Crosato, A. Bonometto, A. Valentini, M. Orlic, I. D. Haigh, J. W. Nielsen, X. Bertin, A. B. Fortunato, B. Pérez Gómez, E. Alvarez Fanjul, D. Paradis, D. Jourdan, A. Pasquet, B. Mourre, J. Tintoré, and R. J. Nicholls, "The prediction of floods in venice: Methods, models and uncertainty," *Natural Hazards and Earth System Sciences Discussions*, pp. 1–47, 2020, ISSN: 1561-8633. DOI: 10.5194/nhess-2020-361. [Online]. Available: https://nhess.copernicus.org/preprints/nhess-2020-361/.

[41] C. Ferrarin, M. Bajo, A. Benetazzo, L. Cavaleri, J. Chiggiato, S. Davison, S. Davolio, P. Lionello, M. Orlić, and G. Umgiesser, "Local and large-scale controls of the exceptional venice floods of november 2019," *Progress in Oceanography*, p. 102 628, 2021, ISSN: 0079-6611. DOI: 10.1016/j.pocean.2021.102628. [Online]. Available: https://www.sciencedirect.com/science/article/pii/S0079661121001142.

[42] L. Cavaleri, M. Bajo, F. Barbariol, M. Bastianini, A. Benetazzo, L. Bertotti, J. Chiggiato, S. Davolio, C. Ferrarin, L. Magnusson, A. Papa, P. Pezzutto, A. Pomaro, and G. Umgiesser, "The october 29, 2018 storm in northern italy – an exceptional event and its modeling," *Progress in Oceanography*, vol. 178, p. 102 178, 2019, ISSN: 0079-6611. DOI: 10.1016/j.pocean.2019.102178. [Online]. Available: https://www.sciencedirect.com/science/article/pii/S0079661119301089.

[43] D. Zanchettin, S. Bruni, F. Raicich, P. Lionello, F. Adloff, A. Androsov, F. Antonioli, V. Artale, E. Carminati, C. Ferrarin, V. Fofonova, R. J. Nicholls, S. Rubinetti, A. Rubino, G. Sannino, G. Spada, R. Thiéblemont, M. Tsimplis, G. Umgiesser, S. Vignudelli, G. Wöppelmann, and S. Zerbini, "Review article: Sea-level rise in venice: Historic and future trends," *Natural Hazards and Earth System Sciences Discussions*, pp. 1–56, 2020, ISSN: 1561-8633. DOI: 10.5194/nhess-2020-351. [Online]. Available: https://nhess.copernicus.org/preprints/nhess-2020-351/.

[44] L. Zampato, M. Bajo, P. Canestrelli, and G. Umgiesser, "Storm surge modelling in venice: Two years of operational results," *Journal of Operational Oceanography*, vol. 9, no. sup1, s46–s57, 2016, ISSN: 1755-876X. DOI: 10.1080/1755876X.2015.1118804.

[45] G. Umgiesser, D. M. Canu, A. Cucco, and C. Solidoro, "A finite element model for the venice lagoon. development, set up, calibration and validation," *Journal of Marine Systems*, vol. 51, no. 1-4, pp. 123–145, 2004, ISSN: 0924-7963. DOI: 10.1016/j.jmarsys.2004.05.009.

[46] A. Roland, A. Cucco, C. Ferrarin, T.-W. Hsu, J.-M. Liau, S.-H. Ou, G. Umgiesser, and U. Zanke, "On the development and verification of a 2-d coupled wave-current model on unstructured meshes," *Journal of Marine Systems*, vol. 78, S244–S254, 2009, ISSN: 0924-7963. DOI: 10.1016/j.jmarsys.2009.01.026.

[47] L. D'Alpaos and A. Defina, "Mathematical modeling of tidal hydrodynamics in shallow lagoons: A review of open issues and applications to the venice lagoon," *Computers & Geosciences*, vol. 33, no. 4, pp. 476–496, 2007, ISSN: 0098-3004. DOI: 10.1016/j.cageo.2006.07.009. [Online]. Available: http://www.sciencedirect.com/science/article/pii/S0098300406001476.

[48] G. Umgiesser, "The impact of operating the mobile barriers in venice (mose) under climate change," *Journal for Nature Conservation*, vol. 54, p. 125 783, 2020, ISSN: 1617-1381. DOI: 10.1016/j.jnc.2019.125783.

[49] C. Ferrarin, A. Tomasin, M. Bajo, A. Petrizzo, and G. Umgiesser, "Tidal changes in a heavily modified coastal wetland," *Continental Shelf Research*, vol. 101, pp. 22–33, 2015, ISSN: 0278-4343. DOI: 10.1016/j.csr.2015.04.002.

[50] R. Cellerino, L. Giancola, and S. Anghinelli, *Venezia atlantide: L'impatto economico delle acque alte*, ser. Economia. Sezione 5, Ricerche di economia applicata. Milano: Angeli, 1998, vol. 80, ISBN: 8846408993.

[51] Deltares, "D-flow flexible mesh user manual,"

[52] R. C. Martyr-Koller, H. Kernkamp, A. van Dam, M. van der Wegen, L. V. Lucas, N. Knowles, B. Jaffe, and T. A. Fregoso, "Application of an unstructured 3d finite volume numerical model to flows and salinity dynamics in the san francisco bay-delta," *Estuarine, Coastal and Shelf Science*, vol. 192, pp. 86–107, 2017, ISSN: 0272-7714. DOI: 10.1016/j.ecss.2017.04.024. [Online]. Available: http://www.sciencedirect.com/science/article/pii/S0272771416307120.

[53] A. Sarretta, S. Pillon, E. Molinaroli, S. Guerzoni, and G. Fontolan, "Sediment budget in the lagoon of venice, italy: Continental shelf research, 30(8), 934-949," *Continental Shelf Research*, vol. 30, no. 8, pp. 934–949, 2010, ISSN: 0278-4343. DOI: 10.1016/J.CSR.2009.07.002.

[54] *Emodnet digital bathymetry (dtm) - european union open data portal*, 2018. [Online]. Available: https://data.europa.eu/euodp/en/data/dataset/EMODnet_bathymetry (visited on).

[55] Learn_ArcGIS, *Map venice in 2d and 3d*, 9/2/2020. [Online]. Available: https://learn.arcgis.com/en/projects/map-venice-in-2d-and-3d/ (visited on).

[56] City of Venice, *Città di venezia — comune di venezia - portale dei servizi*, 2000. [Online]. Available: https://portale.comune.venezia.it/ (visited on).

[57] C. Ferrarin, M. Bajo, and G. Umgiesser, *Model-driven optimization of coastal sea observatories through data assimilation in a finite element hydrodynamic model (SHYFEM v.7_5_65)*. 2020. DOI: 10.5194/gmd-2020-61.

[58] C. Ferrarin, A. Cucco, G. Umgiesser, D. Bellafiore, and C. L. Amos, "Modelling fluxes of water and sediment between venice lagoon and the sea," *Continental Shelf Research*, vol. 30, no. 8, pp. 904–914, 2010, ISSN: 0278-4343. DOI: 10.1016/j.csr.2009.08.014. [Online]. Available: http://www.sciencedirect.com/science/article/pii/S0278434309002544.

[59] J. Ahn, Y. Na, and S. W. Park, "Development of two-dimensional inundation modelling process using mike21 model," *KSCE Journal of Civil Engineering*, vol. 23, no. 9, pp. 3968–3977, 2019, ISSN: 1976-3808. DOI: 10.1007/s12205-019-1586-9.

[60] C. Ferrarin and G. Umgiesser, "Hydrodynamic modeling of a coastal lagoon: The cabras lagoon in sardinia, italy," *Ecological Modelling*, vol. 188, no. 2-4, pp. 340–357, 2005, ISSN: 0304-3800. DOI: 10.1016/j.ecolmodel.2005.01.061. [Online]. Available: http://www.sciencedirect.com/science/article/pii/S0304380005001675.

[61] S. D. Smith and E. G. Banke, "Variation of the sea surface drag coefficient with wind speed," *Quarterly Journal of the Royal Meteorological Society*, vol. 101, no. 429, pp. 665–673, 1975, ISSN: 1477-870X. DOI: 10.1002/qj.49710142920.

[62] K. Bryant and M. Akbar, "An exploration of wind stress calculation techniques in hurricane storm surge modeling," *Journal of Marine Science and Engineering*, vol. 4, no. 3, p. 58, 2016. DOI: 10.3390/jmse4030058. [Online]. Available: https://www.mdpi.com/2077-1312/4/3/58.

[63] I. Kelman and R. Spence, "An overview of flood actions on buildings," *Engineering Geology*, vol. 73, no. 3-4, pp. 297–309, 2004, ISSN: 0013-7952. DOI: 10.1016/j.enggeo.2004.01.010. [Online]. Available: https://www.infona.pl/resource/bwmeta1.element.elsevier-40e04d28-62b4-3c9e-b788-c75d3e640ab6.

[64] H. Patt and R. Jüpner, Eds., *Hochwasser-Handbuch: Auswirkungen und Schutz*, 2. Aufl. 2013. neu bearb. Berlin, Heidelberg: Springer Berlin Heidelberg, 2013, ISBN: 9783642281914. DOI: 10.1007/978-3-642-28191-4.

[65] D. Molinari, A. R. Scorzini, C. Arrighi, F. Carisi, F. Castelli, A. Domeneghetti, A. Gallazzi, M. Galliani, F. Grelot, P. Kellermann, H. Kreibich, G. S. Mohor, M. Mosimann, S. Natho, C. Richert, K. Schroeter, A. H. Thieken, A. P. Zischg, and F. Ballio, "Are flood damage models converging to "reality"? lessons learnt from a blind test," *Natural Hazards and Earth System Sciences*, vol. 20, no. 11, pp. 2997–3017, 2020, ISSN: 1561-8633. DOI: 10.5194/nhess-20-2997-2020. [Online]. Available: https://nhess.copernicus.org/articles/20/2997/2020/nhess-20-2997-2020-discussion.html.

[66] T. Gerl, H. Kreibich, G. Franco, D. Marechal, and K. Schröter, "A review of flood loss models as basis for harmonization and benchmarking," *PLOS ONE*, vol. 11, no. 7, e0159791, 2016, ISSN: 1932-6203. DOI: 10.1371/journal.pone.0159791. [Online]. Available: https://journals.plos.org/plosone/article?id=10.1371/journal.pone.0159791.

[67] Politecnico Milano, *Fdm repository*, 12/11/2020. [Online]. Available: http://www.fdm.polimi.it/models (visited on).

[68] E. Penning-Rowsell, C. Johnson, S. Tunstall, S. Tapsell, J. Morris, J. Chatterton, and C. Green, "The benefits of flood and coastal risk management: A handbook of assessment techniques," *ISBN 1904750516*, 2005. [Online]. Available: https://repository.tudelft.nl/islandora/object/uuid%3A33f2d216-c9bf-419c-b3b1-415a6f6fd881.

[69] Citta di Venezia, *Sistema informativo territoriale*, 8/8/2019. [Online]. Available: http://geoportale.comune.venezia.it/Html5Viewer/index.html?viewer=GeoPortale.Geoportale&LOCALE=IT-it (visited on).

[70] ISTAT, *Basi territoriali e variabili censuarie*, 2020. [Online]. Available: https://www.istat.it/it/archivio/104317 (visited on).

[71] Costo ristrutturazione casa, *Costo ristrutturazione casa venezia: Prezzi dettagliati e preventivi rapidi*, 5/21/2020. [Online]. Available: http://costo-ristrutturazione-casa.it/costo-ristrutturazione-appartamento-venezia/ (visited on).

[72] X. J. Liu, D. H. Zhong, D. W. Tong, Z. Y. Zhou, X. F. Ao, and W. Q. Li, "Dynamic visualisation of storm surge flood routing based on three-dimensional numerical simulation," *Journal of Flood Risk Management*, vol. 11, S729–S749, 2018, ISSN: 1753-318X. DOI: 10.1111/jfr3.12252.

[73] C. Arrighi, M. Brugioni, F. Castelli, S. Franceschini, and B. Mazzanti, "Urban micro-scale flood risk estimation with parsimonious hydraulic modelling and census data," *Natural Hazards and Earth System Sciences*, vol. 13, no. 5, pp. 1375–1391, 2013, ISSN: 1561-8633. DOI: 10.5194/nhess-13-1375-2013. [Online]. Available: https://www.researchgate.net/profile/chiara_arrighi/publication/256430837_urban_micro-scale_flood_risk_estimation_with_parsimonious_hydraulic_modelling_and_census_data.

[74] H. Kreibich, P. Bubeck, M. van Vliet, and H. de Moel, "A review of damage-reducing measures to manage fluvial flood risks in a changing climate," *Mitigation and Adaptation Strategies for Global Change*, vol. 20, no. 6, pp. 967–989, 2015, ISSN: 1573-1596. DOI: 10.1007/s11027-014-9629-5. [Online]. Available: https://link.springer.com/article/10.1007/s11027-014-9629-5.

[75] L. Vergano and Nunes, Paulo A. L. D., "Analysis and evaluation of ecosystem resilience: An economic perspective with an application to the venice lagoon," *Biodiversity and Conservation*, vol. 16, no. 12, pp. 3385–3408, 2007, ISSN: 1572-9710. DOI: 10.1007/s10531-006-9085-y.

[76] N. Tambroni and G. Seminara, "Are inlets responsible for the morphological degradation of venice lagoon?" *Journal of Geophysical Research: Earth Surface*, vol. 111, no. F3, n/a–n/a, 2006, ISSN: 01480227. DOI: 10.1029/2005JF000334. [Online]. Available: https://agupubs.onlinelibrary.wiley.com/doi/full/10.1029/2005JF000334.